MDPI

Article

Impact of Hydrodynamic Cavitation Pretreatment on Sodium Oleate Adsorption onto Diaspore and Kaolinite Surfaces

Weiguang Zhou [1,2], Haobin Wei [3], Yangge Zhu [2], Yufeng Long [1], Yanfei Chen [4,*] and Yuesheng Gao [5,*]

1   Key Laboratory of Coal Processing and Efficient Utilization of Ministry of Education, School of Chemical Engineering and Technology, China University of Mining and Technology, Xuzhou 221116, China; zhouwg2020@cumt.edu.cn (W.Z.); 0305080329@163.com (Y.L.)
2   State Key Laboratory of Mineral Processing, BGRIMM Technology Group, Beijing 102600, China; zhuyangge@bgrimm.com
3   Shandong Bureau of China Metallurgical Geology Bureau, Jinan 250000, China; whbhonor@163.com
4   School of Metallurgy and Environment, Central South University, Changsha 410083, China
5   School of Environment and Resource, Southwest University of Science and Technology, Mianyang 621010, China
*   Correspondence: yanfeichen@csu.edu.cn (Y.C.); ygao4@mtu.edu (Y.G.)

Abstract: To investigate how hydrodynamic cavitation (HC) affects the adsorption of sodium oleate (NaOl) on diaspore and kaolinite surfaces, a comparative study on NaOl adsorption was conducted under different conditions. The flotation and separation of the minerals were also examined with and without HC pretreatment of NaOl. The results show that short-term HC pretreatment of NaOl solutions did not induce a measurable change in the chemical structure of NaOl, but produced micro-nanobubbles (MNBs) and resulted in decreases in the surface tension and viscosity of liquids. When MNBs interacted with minerals, their anchor on solids could affect the contact angles, zeta potentials, and surface NaOl adsorption toward minerals. At low NaOl concentrations, the presence of MNBs reduced the NaOl adsorption capacity and particles' zeta potential while increasing the minerals' contact angle. At higher NaOl concentrations, the presence of MNBs promoted NaOl adsorption, further increased the minerals' contact angle, and further decreases the particles' zeta potential. Additionally, the flotation and separation of minerals can be enhanced at low NaOl concentrations, largely due to the enhanced bubble mineralization through the selective surface-anchoring of MNBs on diaspore. However, the separation efficiency might deteriorate at high NaOl concentrations, though the presence of MNBs amplified the divergences in minerals' surface wettability and zeta potentials.

Keywords: hydrodynamic cavitation; micro-nano bubbles; flotation separation; diaspore; kaolinite

1. Introduction

Froth flotation is an efficient and cost-effective method for separating valuable minerals from gangue minerals. However, its efficiency significantly decreases when the size of the solid particles falls below a certain threshold, primarily due to the reduced collision probability between particles and conventional flotation bubbles [1]. In other words, fine minerals with high specific surface area (SSA) and surface energy present a significant challenge for effective separation and recovery using conventional flotation techniques. To address this issue, several novel flotation technologies have been developed, including shear flocculation flotation, selective flocculation flotation, micro-bubble flotation, etc. [2]. Nonetheless, several drawbacks, such as poor economic benefits, low adaptability, and high reagent consumption, are usually encountered [3]. In contrast, the combination of conventional flotation with hydrodynamic cavitation (HC) has been widely proved to be a promising technique for effectively beneficiating fine minerals [4,5]. One of the reasons for

the success is generally attributed to the micro-nanobubble (MNB) generation during the HC processing [6,7].

MNBs, referred to as tiny bubbles with a size range of several hundred nanometers to sub-microns, typically originate from dissolved gas nuclei or sub-micron to nano-scale gas cavities partially grown from the dissolved gas nuclei in liquids during the HC processing [2,8]. Unlike conventional micro or even larger scale bubbles, MNBs exhibit extraordinary properties, such as long lifetime [9,10], large SSA, high gas solubility [11], etc., which have prompted increased attention in the mineral processing field [12–14]. It has been widely reported that MNBs can significantly enhance the flotation of various minerals, including coal [15], graphite [16], quartz [17], scheelite [18], muscovite [19,20], hematite [21], chalcopyrite [22], rutile [23], molybdenite [24], and others. There are two main contributors to this phenomenon: enhancing fine particle aggregation via MNB bridging [25] and facilitating the bubble mineralization through the pre-anchoring of MNBs on solids [26]. However, the majority of studies have concentrated exclusively on enhancing the flotation enrichment of minerals, paying scant attention to the separation of various minerals in a system involving mineral-neutralized bodies. This oversight presents a pressing issue for industrial applications, particularly in the froth flotation of certain non-ferrous minerals.

The direct flotation process with fatty acid (salt) collectors has shown good adaptability in separating diaspore from other gangue minerals during the beneficiation of diasporic bauxite [27]. The gangue minerals in diasporic bauxite primarily consist of aluminosilicate minerals, such as kaolinite, illite, and pyrophyllite. These minerals are brittle and prone to over-grinding, which leads to the generation of a substantial amount of fine, micro-granular slimes [28,29]. The presence of slime weakens the flotation performances, resulting in poor selection indicators and high reagent consumptions in conventional flotation processes [30]. A high collector consumption also has adverse effects on subsequent backwater utilization and metallurgy [31]. Desliming before flotation can improve bauxite flotation to some extent but may lead to the loss of fine diaspore. Therefore, achieving highly efficient flotation separation of bauxite, recovering fine diaspore particles, and simultaneously reducing reagent consumption is an important issue for researchers. On the other hand, some attempts in enhancing the flotation of diasporic bauxite have been made by introducing MNBs into the flotation system. Under appropriate conditions, this technology achieves significant enhancements in the alumina–silica ratio (A/S) of concentrate while only slightly reducing Al_2O_3 recovery when compared to conventional flotation indicators [32]. However, the impact of MNBs on the flotation separation of primary bauxite ores remains unclear. It is important to note that differences in surface hydrophobicity are necessary for achieving various minerals' separation, and understanding the role of MNBs in different minerals' surface hydrophobization is critical in determining whether this technology can strengthen their separation process. In contrast to the role of MNBs in enhancing fine particle aggregation and bubble mineralization, the role of MNBs in differing the interaction between mineral particles and reagents may be a crucial factor in determining the final separation performance in a MNB flotation system. However, there are currently only a few published reports on the study of the role of MNBs in affecting interactions between mineral particles and reagents, especially on the adsorption of reagents on solids [33,34]. These limitations inevitably hinder our understanding of the role of MNBs in different minerals' flotation separation.

Overall, this study focuses on fine diaspore and kaolinite as the mineral targets, using sodium oleate (NaOl) as the collector. By examining the impact of HC on NaOl solution properties, we investigated how MNBs affect the interaction between solids and NaOl through contact angle measurement, zeta potential determination, and adsorption tests. Ultimately, the flotation separation of fine diaspore and kaolinite was conducted with and without HC pretreatment. Our findings are expected to contribute significantly to understanding the role of MNBs in influencing the flotation separation of various minerals.

2. Experimental

2.1. Mineral Samples and Reagents

Diaspore and kaolinite samples were sourced from the Xiaoguan mine in Henan Province, China, with purity levels exceeding 90%, as confirmed by XRD analysis (Figure 1) and chemical assays (Table 1). The ore was initially crushed, and well-crystallized samples were selected for contact angle measurements. The remaining samples were finely ground using ceramic balls, wet-screened, and subsequently separated to yield products of varying particle sizes. Specifically, the $-10\ \mu m$ fraction was utilized for zeta potential measurements, while the $-37\ \mu m$ fraction was employed in sorption and flotation tests. Table 2 outlines the specific surface areas (SSAs) of these minerals within the $-37\ \mu m$ fraction.
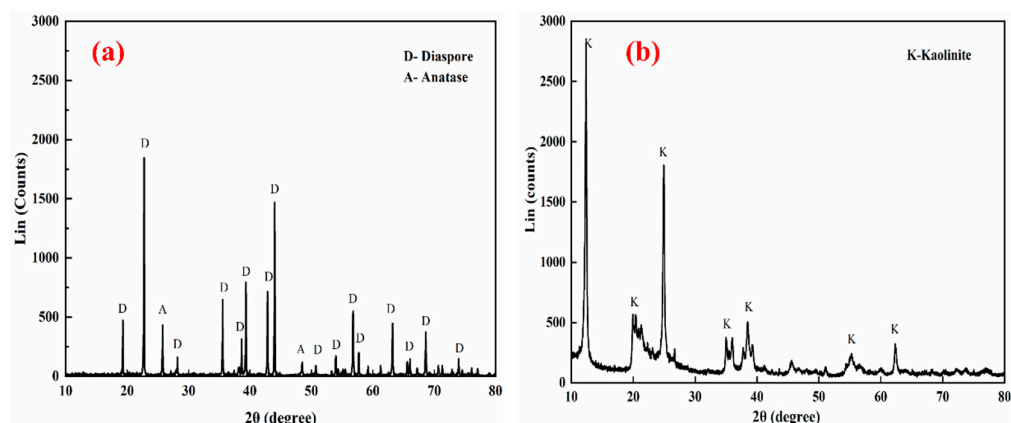

Figure 1. XRD of diaspore (**a**) and kaolinite(**b**) minerals.

Table 1. Chemical composition analysis results.

Composition	Al_2O_3	SiO_2	Fe_2O_3	TiO_2	CaO	MgO	K_2O	Na_2O	Others
Diaspore	70.4	1.21	0.84	8.71	0.02	0.07	0.05	0.04	18.66
Kaolinite	39.61	43.55	0.34	1.86	0.02	0.07	0.01	0.03	14.51

Table 2. SSAs of $-37\ \mu m$ fraction of diaspore and kaolinite particles.

	Diaspore	Kaolinite
SSA (m^2/g)	7.14 ± 0.08	7.76 ± 0.12

The collector used was NaOl (AR grade) procured from Beijing Dingguo Biotechnology Co., Ltd. (Beijing, China). HCl and NaOH were utilized as pH modifiers. Ultrapure water, with a resistivity of 18.2 MΩ·cm, underwent pre-filtration through 0.22 μm microporous membranes prior to use in all experiments.

2.2. HC-Flotation System

Figure 2 schematically shows the HC-flotation system. It consists of a peristaltic pump (WT-600EAS/353Y, JIHPUMP, Chongqing, China) connected to a venturi-type cavitation tube [20], a cavitation reactor, and other components, forming a closed system. Initially, 1400 mL of ultrapure water is mixed with a certain amount of NaOl in the "Container" to prepare a NaOl solution with a specific concentration. After adjusting the pH by HCl and NaOH, the solution is transferred into the "Cavitation reactor". Notably, to eliminate the possible interference of air in the closed system on cavitation, the pipelines and the peristaltic pump are pre-filled by intaking some liquids before the formal HC operation. Afterward, a certain speed of about 16.17 m/s of the peristaltic pump is set to the initial HC for 3 min [32,35], after which the solution is left to stand for a period of time and then transferred for the flotation tests (Direction A1) or other detections (Direction A2).
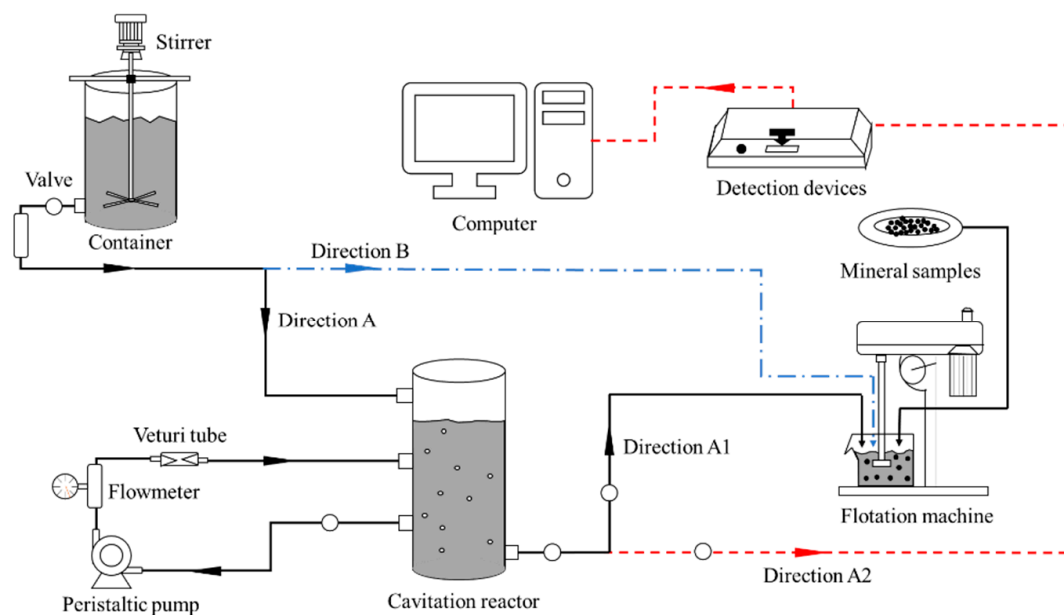
Figure 2. Schematic of HC-flotation system.

2.3. Property Characterization of NaOl Solutions

The infrared spectra of NaOl, both before and after HC pretreatment, were analyzed using an FT-IR spectrometer (740 FT-IR, Nicolet, Waltham, MA, USA), aiming to identify potential chemical modifications caused by HC processing. In each case, a portion of the solution without HC treatment or stagnation for 5 min after HC pretreatment was taken using a pipette and dropped onto a pre-pressed KBr thin slice for infrared spectroscopy detection, with a wavelength measurement range of 4000~400 cm^{-1}. Moreover, a laser particle size analyzer (Mastersizer 2000, Malvern, Grovewood Road, UK) connected to the "Cavitation reactor" was used to measure the size of the possible tiny cavitation bubbles in liquids in situ under different HC conditions [6,22]. Additionally, the surface tension of different solutions was measured using the Wilhelmy Plate method with an automatic tensiometer (JK99D, Shanghai ZhongChen Digital Tech-nic Apparatus Co. Ltd., Shanghai, China). The viscosity of NaOl solutions at different concentrations was also determined using a high-precision rotational rheometer (DHR-2, TA, New Castle, DE, USA). In each experiment, 30 mL of different NaOl solutions were evaluated for viscosity in the rheometer measuring cup. The experimental procedure was carried out using a concentric cylinder standard measurement rotor under linear viscosity mode. Each condition underwent three measurements, and the average value was taken as the final result. All the experiments were carried out at room temperature.

2.4. Contact Angle Measurements

Contact angle measurements were carried out on the surfaces of polished diaspore and kaolinite using the sessile drop method. The well-selected samples were embedded in resin and then sequentially ground with diamond grinding wheels of roughness 100, 40, and 9 μm to achieve a flat surface. Subsequently, the specimens were polished on a micro-cloth using 1.0, 0.3, and 0.05 μm alumina powder solution. After polishing, the specimens were thoroughly washed with ultrapure water and cleaned with a microwave bath to remove any remaining alumina. The specimens were then promptly transferred to a contact angle goniometer (JY-82, Chengde Dingsheng Co., Ltd., Chengde, China) for measurements. Using a calibrated syringe, water droplets were placed, and the contact angles of the samples were measured with different solution additions. The equilibrium contact angle on both sides of the water droplet was measured in five different positions, with the average value being recorded as the final data point.

2.5. Zeta Potential Measurements

The zeta potentials of diaspore and kaolinite particles in different solutions were measured using a Nano ZS 90 particle size analyzer (Malvern, Grovewood Road, UK). For each experiment, 30 mg of the ore sample was first added into 50 mL of differing NaOl solution. After adjusting the pH, it was stirred for 5 min using a magnetic stirrer. Then, the suspension was allowed to settle for 5 min, after which a portion of the upper supernatant was transferred to an electrode groove for zeta potential measurement. Each condition was measured three times repeatedly, using 0.01 M KNO_3 as the background electrolyte, and then the average value was taken as the final reported data point.

2.6. Sorption Experiments

The quantity of NaOl adsorbed onto diaspore and kaolinite surfaces was determined using a high-precision Total Organic Carbon Analyzer (Multi N/C 3100, Analytik Jena, Jena, Germany) across varying conditions. For each trial, 5 g of bauxite or kaolinite ore sample was initially mixed with 95 mL of a specified concentration of NaOl solution in a 150 mL conical flask. This flask was then positioned in a temperature-controlled shaking bath and agitated consistently for 30 min. Subsequently, the mineral suspension underwent centrifugation at 9000 rpm for 15 min, and the resulting supernatant was analyzed to determine the organic carbon content. The concentration of NaOl in the liquid was then calculated using a standard curve, enabling the computation of the amount of NaOl adsorbed onto the mineral surfaces based on the remaining concentration. The adsorption process was conducted thrice for each sample, and an average value was established as the final outcome. The standard deviation had been determined in advance [32].

2.7. Flotation Tests

Flotation tests were carried out using an XFG(II) flotation machine operating at 1400 rpm with a 160 mL cell. In each test, a mineral pulp was prepared by adding 8 g of a single mineral (6.8 g of diaspore and 1.2 g of kaolinite for mixed binary minerals) into the cell along with 152 mL of NaOl solution, both with and without HC pretreatment. The pH of the pulp was adjusted to 10. Following a 3 min conditioning period, flotation was allowed to proceed for 5 min. The floated and unfloated particles were then collected, filtered, and dried. The flotation recovery was calculated based on the distribution of solid mass between the two products. For mixed binary minerals, the aluminum (Al) and silicon (Si) contents were measured, and diaspore recovery was determined based on the distribution of aluminum oxide (Al_2O_3) between the two products. Additionally, the A/S values for both products were calculated.

3. Results and Discussion

3.1. The Effect of HC Pretreatment on the Properties of NaOl Solutions

Figure 3 illustrates the changes in the physiochemical characteristics of NaOl solution induced by HC treatment. In particular, Figure 3a,b display images of the NaOl solution at stages of HC processing completion and after a 5 min cessation of HC treatment, respectively. Obviously, the NaOl solution turned "milky" once HC processing begins, probably due to the generation of numerous tiny cavitation bubbles [36]. After the HC operation, the turbidity of the NaOl solution gradually decreases. However, even after standing for 5 min, the solution does not restore its original clear and transparent appearance. With the extension of standing time, some bubbles in the solution quickly merge and rupture, resulting in a decrease in solution turbidity. Nevertheless, it is believed that those MNBs exhibit exceptional stability in liquids, which causes the decrease in solution's transmittance accordingly [32].
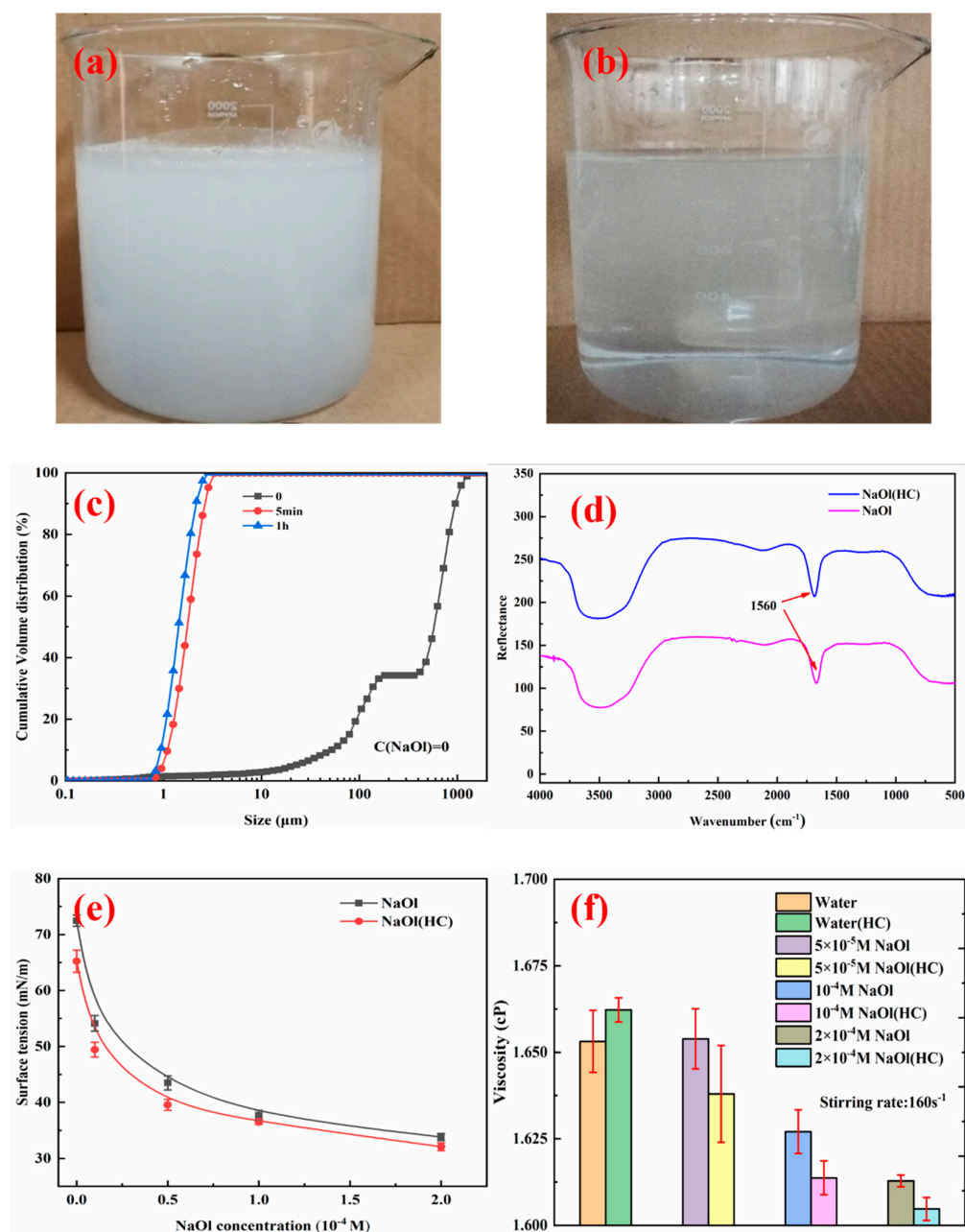
Figure 3. Representative graphs of NaOl solution pretreated by HC and its physicochemical properties ((**a**) NaOl solution once HC stopped; (**b**) NaOl solution stagnating for 5 min after HC; (**c**) size distribution of MNBs in pure water under different stagnation times after HC; (**d**) infrared spectrum of NaOl before and after HC; (**e**) surface tension of NaOl solution before and after HC; (**f**) viscosity of NaOl solution before and after HC under 160 s^{-1}).

Figure 3c presents the distribution of MNBs generated during HC processing in water under different standing times. It is verified that the HC treatment of water results in the production of tiny cavitation bubbles of around several tens of microns in size [22,37]. Upon standing for 5 min, the size distribution curve indicates a significant shift toward smaller ultrafine bubbles with an average size of a few microns present in the liquid. If left to stand for 1 h, the size distribution curve shifts further, albeit to a lesser degree when compared to the 5 min standing time, therefore suggesting that prolonged standing minimally impacts MNB size. This outcome suggests that MNBs possess much greater stability than micro or larger bubbles and can remain stable in pure water for more than 1 h. As a typical surfactant, NaOl can significantly reduce the surface tension of solutions,

which is beneficial to the formation and stability of more and smaller MNBs [38]. Therefore, it is inferred that a large number of MNBs will persist in cavitated NaOl solutions after being left to standing for 5 min.

It is well known that the collapse of tiny cavitation bubbles is normally accompanied by the generation of a large number of hydroxyl radicals during HC. This process is also accompanied by high temperature and pressure, which can probably affect the physico-chemical properties of the solution [39,40]. Thus, we further studied the impact of cavitation on other physicochemical properties of NaOl solution. First, the infrared spectra of NaOl before and after HC treatment were comparatively analyzed, as shown in Figure 3d. The results indicate that the chemical structure of NaOl remained almost unchanged after being treated by HC under the experimental condition. This is likely due to the short duration of the HC treatment, which lasted only 3 min and resulted in lower levels of newly formed hydroxyl radicals and weaker oxidation of NaOl [41]. Then, the impact of HC treatment on the surface tension of NaOl solution was explored and is depicted in Figure 3e. It is evident that the surface tension of the solution indeed reduces after HC treatment, and the reduction rate is even higher when the concentration of NaOl is relatively low. Yasui et al. [42], Bu et al. [43], and Zhou et al. [44] reported similar findings. In addition, the influence of HC treatment on the viscosity of the NaOl solution was investigated (shown in Figure 3f), revealing a slight decrease in viscosity following cavitation treatment. As there are no significant changes in the chemical properties of NaOl during cavitation, it is concluded that the reduction in surface tension and viscosity of NaOl solutions may be attributed to the newly generated MNBs [42]. The presence of MNBs causes an increase in the gas–liquid interface area, which subsequently leads to a decrease in the measured surface tension value. Additionally, fluid viscosity is influenced by internal friction produced by molecular motion transfer and intermolecular attraction during fluid flow at varying velocities. The existence of MNBs transforms a part of the internal friction of the fluid from liquid–liquid interfaces to gas–liquid or gas–gas interfaces, which ultimately results in a decrease in fluid viscosity by reducing interfacial slip resistance [45].

3.2. The Effect of HC Pretreatment on the Interaction between NaOl and Mineral Particles

3.2.1. Effect of Cavitation Treatment of NaOl Solution on Surface Wettability of Diaspore and Kaolinite

The aforementioned results indicate that HC pretreatment does not significantly change the chemical properties of NaOl but promotes the formation of MNBs in the solution. Additionally, due to the decreases in surface tension and viscosity, the liquid spreads and flows more easily on mineral surfaces, which may have a specific impact on the interaction between NaOl and minerals [46]. Figure 4 illustrates the changes in contact angles of diaspore and kaolinite under different conditions with an increase in NaOl concentration. Fresh diaspore has a contact angle of around 27°, reflecting its hydrophilic nature. When interacting with NaOl, the corresponding contact angle of minerals significantly increases with the rise in NaOl concentration due to the enhanced surface hydrophobicity after NaOl adsorption. Notably, the HC pretreatment of NaOl solution leads to a more remarkable contact angle increase, primarily at relatively high NaOl concentrations. The observed increase in contact angle induced by HC pretreatment may be attributed to MNBs generated during HC processing, which can anchor onto mineral surfaces through two types of active sites: inherent geometric defects of solids and chemically induced hydrophobic sites [2]. Moreover, the number of both new stable MNBs formed during cavitation and those chemically induced hydrophobic sites on diaspore surfaces are strongly correlated with NaOl concentration [47]. When the concentration of NaOl is low, fewer stable MNBs may exist in the bulk NaOl solution. Meanwhile, the minimal formation of hydrophobic sites on diaspore surfaces caused by NaOl adsorption do not significantly facilitate the anchoring of MNBs onto surfaces through chemically hydrophobic sites. So, it can be inferred that the enhancement of the contact angle would be attributed to the anchoring of some MNBs at the fine cracks, cavities, and pores on solid surfaces [48]. However, this enhancement

would not be significant in the current case. In contrast, when the concentration of NaOl is relatively high, more MNBs are present in the cavitated solution. Also, the adsorption of NaOl on the surface of diaspore results in the creation of more chemically hydrophobic sites. As a result, more MNBs anchor on the mineral surface with chemically hydrophobic sites as active adsorption sites, leading to a greater increase in the apparent contact angle of diaspore [20,49].
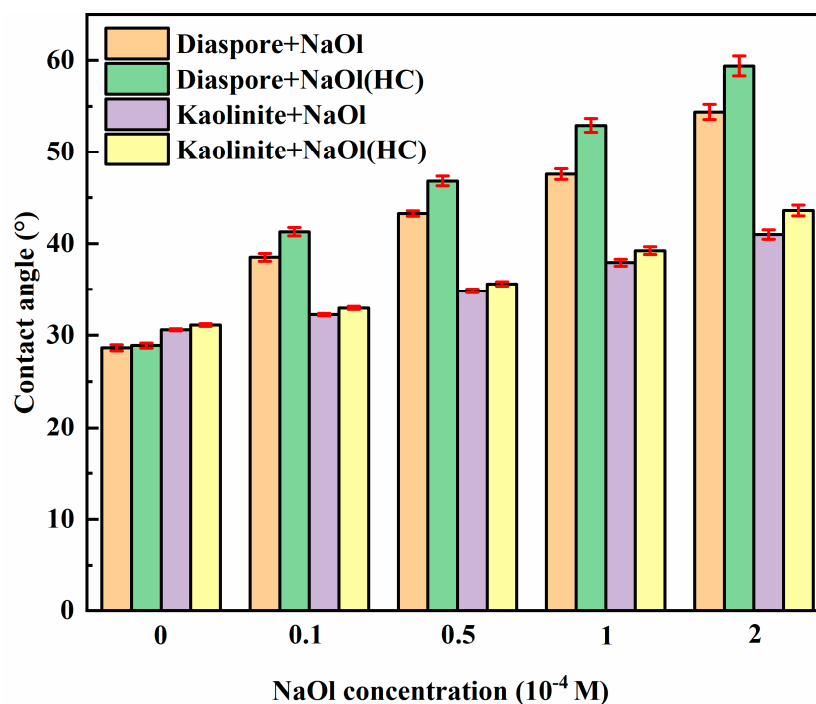

Figure 4. Changes in contact angle of diaspore and kaolinite with NaOl concentrations under different conditions (pH = 10).

Although the natural contact angle of kaolinite is slightly higher than that of diaspore, the growth rate of kaolinite's contact angle after interacting with NaOl is notably lower than that of diaspore. According to Zhang et al. [50], both diaspore and kaolinite achieve surface hydrophobization through the interaction of Al spots on mineral surfaces with NaOl, and the surface abundance of Al in diaspore is 1.7 times greater than that in kaolinite. Therefore, NaOl is more challenging to adsorb on the surface of kaolinite than diaspore. When the concentration of NaOl is less than 0.5×10^{-4} M, regardless of HC pretreatment, the apparent contact angle of kaolinite does not significantly improve following interaction with NaOl. When the concentration of NaOl exceeds 0.5×10^{-4} M, there is a notable increase in the contact angle of kaolinite, regardless of whether HC pretreatment was applied or not. Generally, the trend in the contact angle of kaolinite with increasing NaOl concentration resembles that of diaspore, although the growth in the contact angle of kaolinite is less sensitive to increases in NaOl concentration and HC pretreatment than that of diaspore, especially at relatively low concentrations. As a result, the stably anchoring of MNBs generated during HC processing on hydrophobic sites of minerals may further strengthen the selective surface hydrophobicity of diaspore, which in turn widened the divergence in the surface hydrophobicity between diaspore and kaolinite after interacting with NaOl.

3.2.2. Effect of Cavitation Treatment of NaOl Solution on Zeta Potentials of Diaspore and Kaolinite

Figure 5a depicts the variations in zeta potential of diaspore and kaolinite particles as a function of pH. Initially, valid zeta potential data cannot be obtained in a conventional

NaOl solution where NaOl molecule completely ionizes. However, after treating the NaOl solution with HC, highly negatively charged colloids are detected, which are primarily newborn organic-armored MNBs generated in the HC process [7]. Meanwhile, the surface potentials of kaolinite and diaspore particles significantly shift to negative as pH increases. Diaspore's isoelectric point is around 7.5, while kaolinite's is about 4.3. The addition of NaOl leads to a noticeable decrease in the zeta potential of both minerals, indicating the adsorption of NaOl on their surfaces. However, the HC pretreatment of NaOl solution results in a reduction in the movement in the negative direction of zeta potential of diaspore particles across the experimental pH range. Similarly, the negative movement of kaolinite's zeta potential curve decreases when pH exceeds 8.5 in the presence of HC pretreatment. The presence of charged MNBs significantly affects the electrokinetic properties of different interfaces [51,52], likely causing the reduction in zeta potential of the two minerals due to MNB anchoring on their surfaces. This reduction in zeta potential may occur through mechanisms such as steric hindrance, electric double-layer (EDL) overlapping, and ion shielding [53]. However, the reduction degree of zeta potential of diaspore caused by HC pretreatment is significantly higher than that of kaolinite at pH 10. This suggests that the interaction between MNBs and diaspore particles is stronger, and there seems to be more MNBs stably anchored at diaspore surfaces than kaolinite at pH 10. These findings are consistent with the contact angle data mentioned above.
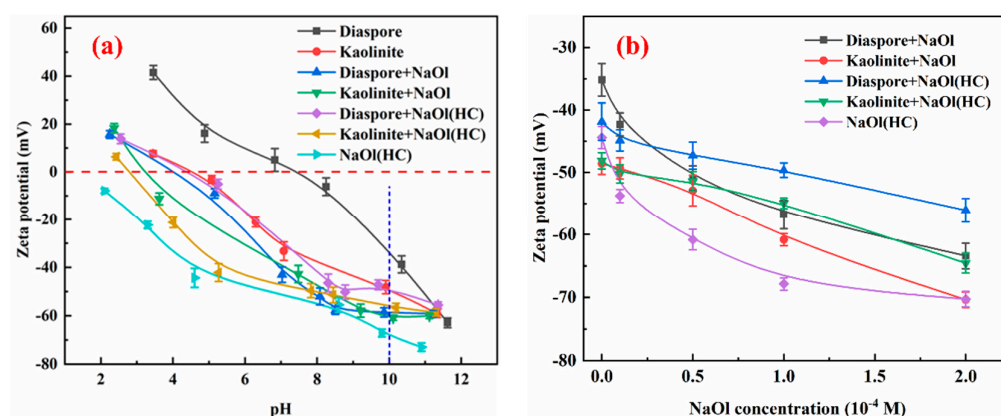

Figure 5. Changes in zeta potential of colloids in diaspore and kaolinite pulps under different conditions ((**a**) C(NaOl) = 10^{-4} M; (**b**) pH = 10).

To further explore the impact of HC pretreatment on the minerals' zeta potential, changes in the minerals' zeta potential with varying NaOl concentrations were examined under pH 10 (shown in Figure 5b). Evidently, diaspore, kaolinite and MNBs are all negatively charged in pure water at pH 10. However, the surface of kaolinite is more negatively charged than that of diaspore, suggesting stronger electrostatic repulsion between kaolinite and MNBs. This creates a larger electrostatic energy barrier that inhibits collision and adhesion between kaolinite and MNBs, which may be another reason why MNBs adhere more easily to the surface of diaspore than kaolinite.

Moreover, at low NaOl concentrations (i.e., $\leq 0.5 \times 10^{-4}$ M), the HC pretreatment causes a significant positive shift in diaspore's zeta potential, while imposing only a negligible effect on kaolinite. This reconfirms that the interaction between MNBs and diaspore is more substantial than that between MNBs and kaolinite. In this case, MNBs are likely to attach themselves to the surface of diaspore, reducing its zeta potential through the "steric hindrance" effect, EDL overlapping, and ion shielding. However, it is difficult for MNBs to stably anchor at the surface of kaolinite. Instead, most MNBs tend to remain suspended in bulks. While free bulk MNBs can also impact the determination of kaolinite potential through DEL compression, this effect is generally insignificant as per our previous research [53].

When the concentration of NaOl exceeds 1×10^{-4} M, the zeta potential of both diaspore and kaolinite decreases after pretreating the NaOl solution with HC. Higher concentrations of NaOl lead to the formation of more chemically hydrophobic sites for MNBs to latch onto, which results in more MNBs being stably anchored to the minerals' surfaces, consequently decreasing the measured zeta potential values. However, even in this case, the zeta potential of diaspore still decreases more significantly than that of kaolinite. This implies that, although MNBs can effectively anchor onto the surface of both minerals at higher NaOl concentrations, a greater number of MNBs are likely to be anchored onto the surface of diaspore. Additionally, the reduction in the zeta potential of solids caused by MNBs anchoring on mineral surfaces is more significant than the increase in the particles' zeta potential induced by NaOl adsorption.

3.2.3. Effect of Cavitation Pretreatment on Adsorption Capacity of NaOl on Diaspore and Kaolinite

After anchoring to mineral surfaces, MNBs occupy a certain space on the mineral's surfaces. Numerous studies have shown that the anchoring of MNBs on mineral surfaces inevitably affects the chemical reagent adsorption on solids, although detailed explanations are still lacking. Some reports suggest that MNBs may diminish the adsorption ability of reagents on mineral surfaces by hindering their direct adsorption [38,54], leading to a decrease in minerals' zeta potential [51]. However, other studies have proposed that MNBs' existence may not lower the reagent adsorption but instead transforms some of the reagents from assembling at the solid–liquid interface to gas–liquid–solid or even gas–liquid interface [55–58]. Therefore, a quantitative comparison was conducted to determine how HC and associated MNBs affect NaOl adsorption on mineral surfaces by assessing differences in the quantity of NaOl present on mineral surfaces.

Figure 6 illustrates the adsorption of NaOl on diaspore and kaolinite particles under different conditions. Figure 6a shows that increasing NaOl concentration directly increases the amount of NaOl adsorbed on both minerals. The adsorption of NaOl on solids is notably influenced by HC pretreatment, leading to a substantial increase in adsorption at higher initial NaOl concentrations. These observations corroborate well with the outcomes of contact angle and zeta potential tests. Since the adsorption data were quantitively obtained using the residual concentration method, this finding additionally suggests that more NaOl molecules accumulate on the solid–MNB aggregates, most likely through a combination of direction adsorption (adsorption occurs at the solid–liquid interface), gas-vapor deposition [59], or assembling at MNB surfaces in cavitated solutions [60–62].
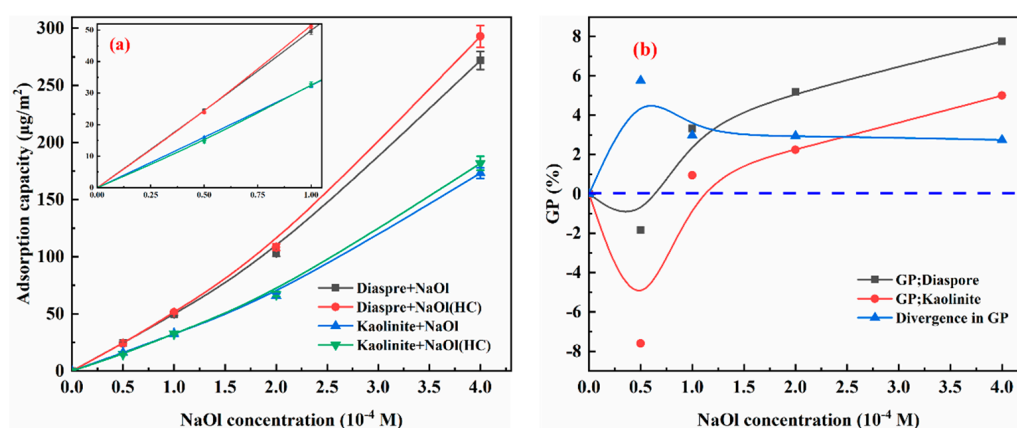

Figure 6. Adsorption of NaOl on the surfaces of fine diaspore and kaolinite under different conditions ((**a**) Adsorption capacity Vs NaOl concentration; (**b**) GP Vs NaOl concentration; pH = 10).

More quantitative details about the growth rate of NaOl adsorption on mineral surfaces induced by HC pretreatment (i.e., GP) are displayed in Figure 6b. The calculation of GP is based on the following formula:

$$GP = (A_{NaOl(HC)} - A_{NaOl})/A_{NaOl} \times 100\%$$

where $A_{NaOl(HC)}$ represents the quantity of NaOl adsorbed on mineral surfaces in cavitated NaOl solutions, and A_{NaOl} represents the amount of NaOl adsorbed on mineral surfaces in conventional NaOl solutions. For each single mineral, the GP values decline initially and then rises quickly before gradually reaching an endpoint, as the level of NaOl increases. Specifically, when the concentration of NaOl is low (around 0.5×10^{-4} M), the corresponding GP values for both minerals are negative, indicating that the HC pretreatment reduces the adsorption amount of NaOl on mineral surfaces. The introduction of MNBs during the HC processing creates abundant gas–liquid interfaces in liquids. As a result, some NaOl molecules may accumulate on the surfaces of these tiny bubbles instead of interacting with the mineral interface. Moreover, only a few chemically hydrophobic sites can be formed on mineral surfaces, making it unfavorable for the stable anchoring of NaOl-armored MNBs [47]. Thus, the low concentration of NaOl, combined with HC pretreatment, leads to a reduction in the amount of NaOl adsorbed on mineral-MNBs aggregates, which therefore contributes to the reduction in the measured zeta potential of solids.

In contrast, at higher NaOl concentrations, the GP values rapidly increase to be positive, indicating that HC pretreatment increases the adsorption capacity of NaOl on mineral surfaces. However, despite the increase in GP value, the measured zeta potential still declines gradually. This implies that some organic molecules may interact with solids through adsorption at the gas–liquid interface, and the zeta potential reduction caused by MNBs anchoring on solids may take precedence. In addition, the divergence in GP values between diaspore and kaolinite displays an initial increase followed by a slow decrease trend with a maximum obtained at a concentration of 0.5×10^{-4} M. Based on the data about contact angle and NaOl adsorption on mineral surfaces, this finding implies that the increase in the measured contact angle may be associated not only with the amount of NaOl adsorbed on the mineral surface but also with the geometric heterogeneity of anchored MNBs.

In summary, the interaction between NaOl and minerals leads to the formation of chemically hydrophobic sites on their surfaces. MNBs generated during HC processing may impose varying influences on contact angles, zeta potentials, and surface NaOl adsorption toward minerals at different NaOl concentrations. At low NaOl concentrations ($<0.5 \times 10^{-4}$ M), the presence of MNBs may not be favorable for the adsorption of NaOl on both minerals, causing a reduction in particles' zeta potential due to lower NaOl adsorption. The increase in the mineral's contact angle could be mainly due to the geometric heterogeneity of anchored MNBs on solids. However, at high NaOl concentrations, the presence of MNBs improves the NaOl adsorption on both minerals, attributing to increased NaOl adsorption and the heterogeneity of anchored MNBs on solids. The measured contact angle of minerals is noticeably increased under these conditions. Despite this improvement, the detected zeta potential of mineral particles still gradually decreases, possibly due to the significant number of anchored MNBs on solids, which reduce the particles' zeta potential through the steric hindrance effect, EDL overlapping, and ion shielding. Figure 7 depicts a possible model of NaOl adsorption on diaspore and kaolinite surfaces with and without HC pretreatment of NaOl solutions.
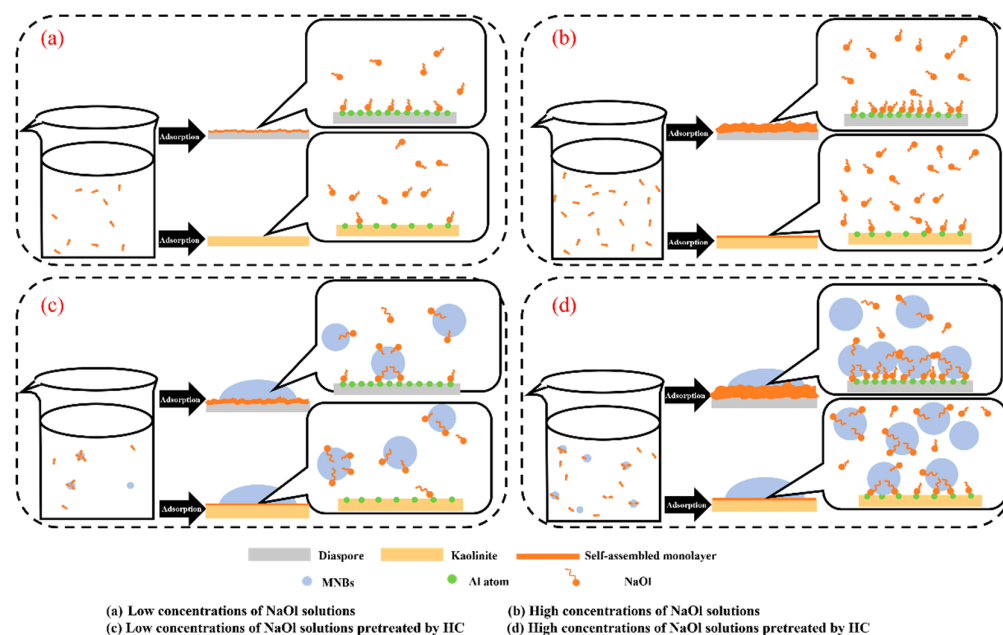
Figure 7. Schematic of the adsorption of NaOl on the surfaces of diaspore and kaolinite in the absence and presence of HC pretreatment.

3.3. The Effect of HC Pretreatment on the Flotation Separation of Fine Diaspore and Kaolinite

The HC pretreatment of NaOl solutions has a positive effect on increasing the surface hydrophobicity of minerals and decreasing the zeta potential of particles, which are important factors for mineral flotation and separation. In Figure 8a, the recovery of both diaspore and kaolinite increases with increasing NaOl concentration and HC pretreatment, confirming that MNBs can act as secondary collectors for flotation [17]. However, the effect of HC pretreatment on diaspore flotation diminishes as NaOl concentration increases, while for kaolinite, HC pretreatment has the greatest promoting effect when the NaOl concentration is between 0.5×10^{-4} and 1×10^{-4} M. Through combing the data from Section 3.2, it can be seen that at low-to-medium NaOl concentrations, HC pretreatment dose not significantly enhance the mineral's surface contact angle, reduce the particle's zeta potential, or increase NaOl adsorption. Consequently, particle bridging induced by MNBs is not thought to be very significant. Conversely, the improved mineralization of bubbles assisted by surface-anchoring MNBs is likely the key contributor for the enhanced flotation of minerals at these concentrations. At high NaOl concentrations, the role of MNBs in promoting NaOl adsorption on solid–MNB aggregates, which improves the surface hydrophobicity of minerals and reducing the zeta potential of the particles, tends to be increasingly noticeable, which also contributes to the enhancement in the flotation enrichment of minerals. However, as the concentration of NaOl increases, the HC pretreatment and accompanying MNB-enhanced flotation enrichment gradually weaken, which at least suggests that the strengthening effect of MNBs on flotation enrichment mainly results from the enhanced bubble mineralization aspect in the present flotation system.
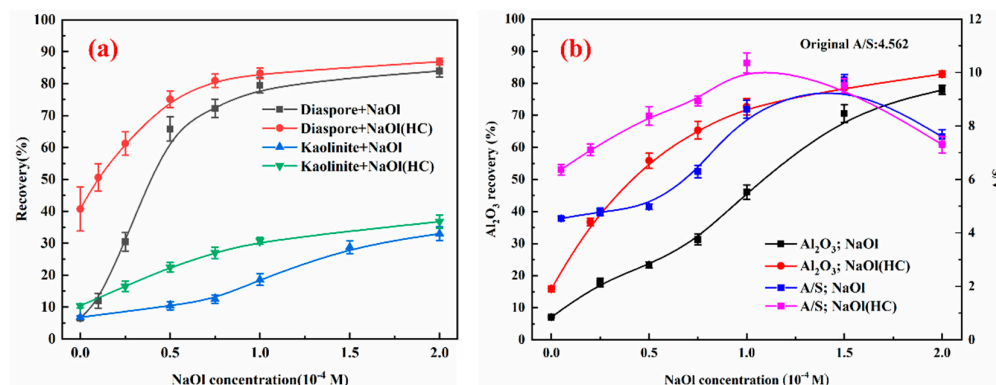
Figure 8. Flotation and separation of diaspore and kaolinite with and without HC pretreatment of NaOl solutions ((**a**) Diaspore/kaolinite flotation recovery Vs NaOl concentrations; (**b**) Flotation separation performance of diaspore and kaolinite artificial mixture Vs NaOl concentrations; pH = 10).

HC pretreatment displays promising potential in effectively enhancing the flotation separation of diaspore and kaolinite, particularly at low NaOl concentrations. To determine the actual influence of HC pretreatment on the separation of fine diaspore from fine kaolinite, the flotation separation of the minerals' mixture under varying NaOl concentrations was explored, with the indicators of concentrate shown in Figure 8b. Obviously, HC pretreatment significantly improves the Al_2O_3 recovery in concentration across the experimental NaOl range, achieving maximum enhancement between 0.5×10^{-4} M and 1×10^{-4} M NaOl concentration. When compared with conventional flotation, it is observed that flotation with HC pretreatment produces higher A/S in concentration when NaOl concentration is below 1.5×10^{-4} M. However, when NaOl concentration exceeds 1.5×10^{-4} M, the A/S witnesses a slight decline after HC pretreatment. Therefore, under appropriate NaOl concentration conditions, HC pretreatment of NaOl solution can effectively enhance the flotation and separation of fine diaspore and kaolinite, while simultaneously achieving higher Al_2O_3 recovery and the final A/S concentration.

When interacting with minerals, NaOl exhibits a stronger affinity toward diaspore than kaolinite, resulting in more anchored MNBs on the surface of diaspore due to the ease of MNBs anchoring on a more hydrophobic surface. At low concentrations of NaOl, a small number of MNBs can stably anchor on the surface of diaspore, while almost no MNBs can stably anchor on kaolinite surfaces. Although there seems to be no significant change in macroscopic wettability and the zeta potential of mineral particles induced by MNBs at this case, the selective attachment of MNBs on mineral surfaces leads to a selective improvement in bubble mineralization between these two minerals, which is likely responsible for the high selectivity of the final flotation separation. At relatively high concentrations of NaOl, the selective anchoring of MNBs on solids amplifies the differences in macroscopic wettability and zeta potential between diaspore and kaolinite particles while maintaining a relatively constant divergence in the adsorption amount of NaOl, and the corresponding separation performance sharply deteriorates. This may be due to the high concentrations of NaOl and MNBs present in the system, which causes an overall drop in the separation selectivity of the flotation in final.

It is noteworthy that under low NaOl concentration conditions, the significant differences observed in flotation recovery and separation between fine diaspore and kaolinite are likely attributable to the selective enhancement of bubble mineralization in diaspore, facilitated by the selective surface-anchoring of MNBs. However, direct supporting evidence is currently lacking, prompting further research. In summary, this study constitutes a preliminary investigation, highlighting the need for further extensive research to attain a comprehensive understanding of NaOl adsorption and assembly on surfaces of diverse minerals. Such understanding is crucial for deciphering the intricate interface interactions in HC or MNB-assisted flotation applications.

4. Conclusions

Based on the results, the following conclusions can be drawn:

1. Short-term (3 min) HC treatment does not noticeably change the chemical properties of NaOl but promotes the formation of MNBs in liquids, which therefore causes certain reductions in surface tension and viscosity of NaOl solutions.

2. At low NaOl concentrations, the presence of MNBs generated during HC processing hinders the adsorption of NaOl on mineral surfaces, resulting in a decrease in the zeta potential of mineral particles. However, the macroscopic contact angle of solids can still be enlarged slightly, probably due to the geometric heterogeneity of anchored MNBs on mineral surfaces.

3. At relatively high NaOl concentrations, the introduction of MNBs promotes the adsorption of NaOl on mineral–MNB aggregates, leading to a significant increase in the macroscopic contact angles of solids. But it still causes a reduction in the measured zeta potential of solids, probably due to the "steric hindrance" effect, EDL overlapping, and ion shielding induced by anchored MNBs on mineral surfaces.

4. The pretreatment of NaOl solution with HC can enhance the flotation enrichment of both fine diaspore and kaolinite across the experimental NaOl concentration range, while the separation of these minerals can only be improved at relatively low NaOl concentrations. The newly generating and surface anchoring of MNBs benefit the mineral particle aggregation and bubble mineralization, all of which lead to the increased flotation enrichment of the minerals. Nonetheless, it appears that MNB-enhanced bubble mineralization may play a more important role in facilitating the flotation separation of diaspore and kaolinite under the current system.

Author Contributions: W.Z.: methodology, formal analysis, data curation, investigation, and writing—original draft. H.W. and Y.Z.: conceptualization, formal analysis, investigation, and writing—review and editing. Y.L.: formal analysis, supervision, and project administration. Y.C.: resources and project administration. Y.G.: resources and investigation. All authors have read and agreed to the published version of the manuscript.

Data Availability Statement: Data will be made available on request.

Conflicts of Interest: The authors declare that they have no known competing financial interests or personal relationships that could have appeared to influence the work reported in this paper.

References

1. Crawford, R.; Ralston, J. The influence of particle size and contact angle in mineral flotation. *Int. J. Miner. Process.* **1988**, *23*, 1–24. [CrossRef]
2. Zhou, Z.A.; Xu, Z.; Finch, J.A.; Masliyah, J.H.; Chow, R.S. On the role of cavitation in particle collection in flotation—A critical review. II. *Miner. Eng.* **2009**, *22*, 419–433. [CrossRef]
3. Li, C.; Xu, M.; Xing, Y.; Zhang, H.; Peuker, U.A. Efficient separation of fine coal assisted by surface nanobubbles. *Sep. Purif. Technol.* **2020**, *249*, 117163. [CrossRef]
4. Fan, M.; Tao, D.; Honaker, R.; Luo, Z. Nanobubble generation and its applications in froth flotation (part III): Specially designed laboratory scale column flotation of phosphate. *Min. Sci. Technol.* **2010**, *20*, 317–338. [CrossRef]
5. Fan, M.; Tao, D.; Honaker, R.; Luo, Z. Nanobubble generation and its applications in froth flotation (part IV): Mechanical cells and specially designed column flotation of coal. *Min. Sci. Technol.* **2010**, *20*, 641–671. [CrossRef]
6. Fan, M.; Tao, D.; Honaker, R.; Luo, Z. Nanobubble generation and its application in froth flotation (part I): Nanobubble generation and its effects on properties of microbubble and millimeter scale bubble solutions. *Min. Sci. Technol.* **2010**, *20*, 1–19. [CrossRef]
7. Calgaroto, S.; Wilberg, K.Q.; Rubio, J. On the nanobubbles interfacial properties and future applications in flotation. *Miner. Eng.* **2014**, *60*, 33–40. [CrossRef]

8. Oliveira, H.; Azevedo, A.; Rubio, J. Nanobubbles generation in a high-rate hydrodynamic cavitation tube. *Miner. Eng.* **2018**, *116*, 32–34. [CrossRef]

9. Tan, B.H.; An, H.; Ohl, C.D. Stability of surface and bulk nanobubbles. *Curr. Opin. Colloid In.* **2021**, *53*, 101428. [CrossRef]

10. Sun, Y.; Xie, G.; Peng, Y.; Xia, W.; Sha, J. Stability theories of nanobubbles at solid–liquid interface: A review. *Colloid Surface A* **2016**, *495*, 176–186. [CrossRef]

11. German, S.R.; Wu, X.; An, H.; Craig, V.S.J.; Mega, T.L.; Zhang, X. Interfacial nanobubbles are leaky: Permeability of the gas/water interface. *ACS Nano* **2014**, *8*, 6193–6201. [CrossRef] [PubMed]

12. Azevedo, A.; Oliveira, H.; Rubio, J. Bulk nanobubbles in the mineral and environmental areas: Updating research and applications. *Adv. Colloid Interface* **2019**, *271*, 101992. [CrossRef] [PubMed]

13. Alheshibri, M.; Qian, J.; Jehannin, M.; Craig, V.S.J. A history of nanobubbles. *Langmuir* **2016**, *32*, 11086–11100. [CrossRef] [PubMed]

14. Zhang, F.; Sun, L.; Yang, H.; Gui, X.; Schönherr, H.; Kappl, M.; Cao, Y.; Xing, Y. Recent advances for understanding the role of nanobubbles in particles flotation. *Adv. Colloid Interface* **2021**, *291*, 102403. [CrossRef] [PubMed]

15. Xing, Y.; Gui, X.; Cao, Y.; Wang, D.; Zhang, H. Clean low-rank-coal purification technique combining cyclonic-static microbubble flotation column with collector emulsification. *J. Clean. Prod.* **2017**, *153*, 657–672. [CrossRef]

16. Tang, C.; Wu, T.; Zhang, D.; Wang, Y.; Zhao, T.; Fan, Z.; Liu, X. Study on surface physical and chemical mechanism of nanobubble enhanced flotation of fine graphite. *J. Ind. Eng. Chem.* **2023**, *122*, 389–396.

17. Calgaroto, S.; Azevedo, A.; Rubio, J. Flotation of quartz particles assisted by nanobubbles. *Int. J. Miner. Process.* **2015**, *137*, 64–70. [CrossRef]

18. Zhou, W.; Chen, H.; Ou, L.; Shi, Q. Aggregation of ultra-fine scheelite particles induced by hydrodynamic cavitation. *Int. J. Miner. Process.* **2016**, *157*, 236–240. [CrossRef]

19. Chen, G.; Ren, L.; Zhang, Y.; Bao, S. Improvement of fine muscovite flotation through nanobubble pretreatment and its mechanism. *Miner. Eng.* **2022**, *189*, 107868. [CrossRef]

20. Zhou, W.; Niu, J.; Xiao, W.; Ou, L. Adsorption of bulk nanobubbles on the chemically surface-modified muscovite minerals. *Ultrason. Sonochem.* **2019**, *51*, 31–39. [CrossRef]

21. Tao, D.; Wu, Z.; Sobhy, A. Investigation of nanobubble enhanced reverse anionic flotation of hematite and associated mechanisms. *Powder. Technol.* **2021**, *379*, 12–25. [CrossRef]

22. Ahmadi, R.; Khodadadi, D.A.; Abdollahy, M.; Fan, M. Nano-microbubble flotation of fine and ultrafine chalcopyrite particles. *Int. J. Min. Sci. Technol* **2014**, *24*, 559–566. [CrossRef]

23. Zhang, Z.; Ren, L.; Zhang, Y. Role of nanobubbles in the flotation of fine rutile particles. *Miner. Eng.* **2021**, *172*, 107140. [CrossRef]

24. Wang, X.; Yuan, S.; Liu, J.; Zhu, Y.; Han, Y. Nanobubble-enhanced flotation of ultrafine molybdenite and the associated mechanism. *J. Mol. Liq.* **2022**, *346*, 118312. [CrossRef]

25. Hampton, M.A.; Nguyen, A.V. Nanobubbles and the nanobubble bridging capillary force. *Adv. Colloid Interface* **2010**, *154*, 30–55. [CrossRef]

26. Zhang, F.; Xing, Y.; Chang, G.; Yang, Z.; Cao, Y.; Gui, X. Enhanced lignite flotation using interfacial nanobubbles based on temperature difference method. *Fuel* **2021**, *293*, 120313. [CrossRef]

27. Wang, Y.; Feng, Y.; Zhang, Q.; Lu, D.; Hu, Y. Flotation separation of diaspore from aluminosilicates using commercial oleic acids of different iodine values. *Int. J. Miner. Process.* **2017**, *168*, 95–101. [CrossRef]

28. Hu, Y.; Liu, X.; Xu, Z. Role of crystal structure in flotation separation of diaspore from kaolinite, pyrophyllite and illite. *Miner. Eng.* **2003**, *16*, 219–227. [CrossRef]

29. Xu, L.; Hu, Y.; Dong, F.; Gao, Z.; Wu, H.; Wang, Z. Anisotropic adsorption of oleate on diaspore and kaolinite crystals: Implications for their flotation separation. *Appl. Surf. Sci.* **2014**, *321*, 331–338. [CrossRef]

30. Yin, W.; Wang, J. Effects of particle size and particle interactions on scheelite flotation. *Trans. Nonferrous Met. Soc.* **2014**, *24*, 3682–3687. [CrossRef]

31. Gibson, B.; Wonyen, D.G.; Chelgani, S.C. A review of pretreatment of diasporic bauxite ores by flotation separation. *Miner. Eng.* **2017**, *114*, 64–73. [CrossRef]

32. Zhou, W.; Liu, K.; Wang, L.; Zhou, B.; Niu, J.; Ou, L. The role of bulk micro-nanobubbles in reagent desorption and potential implication in flotation separation of highly hydrophobized minerals. *Ultrason. Sonochem.* **2020**, *64*, 104996. [CrossRef] [PubMed]

33. Wang, Y.; Pan, Z.; Jiao, F.; Qin, W. Understanding bubble growth process under decompression and its effects on the flotation phenomena. *Miner. Eng.* **2020**, *145*, 106066. [CrossRef]

34. Owens, C.L.; Schach, E.; Rudolph, M.; Nash, G.R. Surface nanobubbles on the carbonate mineral dolomite. *Rsc. Adv.* **2018**, *8*, 35448–35452. [CrossRef]

35. Li, H.; Afacan, A.; Liu, Q.; Xu, Z. Study interactions between fine particles and micron size bubbles generated by hydrodynamic cavitation. *Miner. Eng.* **2015**, *84*, 106–115. [CrossRef]

36. Etchepare, R.; Oliveira, H.; Nicknig, M.; Azevedo, A.; Rubio, J. Nanobubbles: Generation using a multiphase pump, properties and features in flotation. *Miner. Eng.* **2017**, *112*, 19–26. [CrossRef]

37. Couto, H.J.B.; Nunes, D.G.; Neumann, R.; França, S.C.A. Micro-bubble size distribution measurements by laser diffraction technique. *Miner. Eng.* **2009**, *22*, 330–335. [CrossRef]

38. Wang, Y.; Pan, Z.; Luo, X.; Qin, W.; Jiao, F. Effect of nanobubbles on adsorption of sodium oleate on calcite surface. *Miner. Eng.* **2019**, *133*, 127–137. [CrossRef]

39. Minamoto, C.; Fujiwara, N.; Shigekawa, Y.; Tada, K.; Yano, J.; Yokoyama, T.; Minamoto, Y.; Nakayama, S. Effect of acidic conditions on decomposition of methylene blue in aqueous solution by air microbubbles. *Chemosphere* **2021**, *263*, 128141. [CrossRef]

40. Takahashi, M.; Chiba, K.; Li, P. Free-radical generation from collapsing microbubbles in the absence of a dynamic stimulus. *J. Phys. Chem. B* **2007**, *111*, 1343–1347. [CrossRef]

41. Yang, L.; Li, X.; Li, W.; Yan, X.; Zhang, H. Intensification of interfacial adsorption of dodecylamine onto quartz by ultrasonic method. *Sep. Purif. Technol.* **2019**, *227*, 115701. [CrossRef]

42. Yasui, K.; Tuziuti, T.; Izu, N.; Kanematsu, W. Is surface tension reduced by nanobubbles (ultrafine bubbles) generated by cavitation? *Ultrason. Sonochem.* **2019**, *52*, 13–18. [CrossRef] [PubMed]

43. Bu, X.; Zhou, S.; Tian, X.; Ni, C.; Nazari, S.; Alheshibri, M. Effect of aging time, airflow rate, and nonionic surfactants on the surface tension of bulk nanobubbles water. *J. Mol. Liq.* **2022**, *359*, 119274. [CrossRef]

44. Zhou, S.; Nazari, S.; Hassanzadeh, A.; Bu, X.; Ni, C.; Peng, Y.; Xie, G.; He, Y. The effect of preparation time and aeration rate on the properties of bulk micro-nanobubble water using hydrodynamic cavitation. *Ultrason. Sonochem.* **2022**, *84*, 105965. [CrossRef] [PubMed]

45. Li, X.X.; Guo, X.F.; Zhang, M.; Zhang, H.W.; Wang, Y.W.; Chao, S.L.; Ren, H.T.; Wu, S.H.; Jia, S.Y.; Liu, Y.; et al. Enhanced permeate flux by air micro-nano bubbles via reducing apparent viscosity during ultrafiltration process. *Chemosphere* **2022**, *302*, 134782. [CrossRef]

46. Kang, W.Z.; Xun, H.X.; Kong, X.H.; Li, M.M. Effects from changes in pulp nature after ultrasonic conditioning on high-sulfur coal flotation. *Min. Sci. Technol.* **2009**, *19*, 498–507. [CrossRef]

47. Lu, L.A.C.; Klitzing, R.V. Scanning of silicon wafers in contact with aqueous CTAB solutions below the CMC. *Langmuir* **2012**, *28*, 3360–3368.

48. Xing, Y.; Zhang, Y.; Liu, M.; Xu, M.; Guo, F.; Han, H.; Gao, Z.; Cao, Y.; Gui, X. Improving the floatability of coal with varying surface roughness through hypobaric treatment. *Powder Technol.* **2019**, *345*, 643–648. [CrossRef]

49. Zhou, W.; Wu, C.; Lv, H.; Zhao, B.; Liu, K.; Ou, L. Nanobubbles heterogeneous nucleation induced by temperature rise and its influence on minerals flotation. *Appl. Surf. Sci.* **2020**, *508*, 145282. [CrossRef]

50. Zhang, G.; Feng, Q.; Lu, Y.; Ou, L. Mechanism on diaspore and kaolinite collected by sodium oleate. *Chin. J. Nonferrous. Met.* **2001**, *11*, 4. (In Chinese)

51. Churaev, N.V.; Ralston, J.; Sergeeva, I.P.; Sobolev, V.D. Electrokinetic properties of methylated quartz capillaries. *Adv. Colloid Interface* **2002**, *96*, 265–278. [CrossRef] [PubMed]

52. Snoswell, D.R.E.; Duan, J.; Fornasiero, D.; Ralston, J. Colloid stability and the influence of dissolved gas. *J. Phys. Chem. B* **2003**, *107*, 2986–2994. [CrossRef]

53. Zhou, W.; Liu, L.; Zhou, B.; Weng, L.; Li, J.; Liu, C.; Yang, S.; Wu, C.; Liu, K. Electrokinetic potential reduction of fine particles induced by gas nucleation. *Ultrason. Sonochem.* **2020**, *67*, 105167. [CrossRef] [PubMed]

54. Pourkarimi, Z.; Rezai, B.; Noaparast, M.; Nguyen, A.V.; Chelgani, S.C. Proving the existence of nanobubbles produced by hydrodynamic cavitation and their significant effects in powder flotation. *Adv. Powder. Technol.* **2021**, *32*, 1810–1818. [CrossRef]

55. Seo, H.; Ko, W.; Jeon, S. Influence of dissolved air on the adsorption properties and stability of vesicles on various surfaces. *Appl. Phys. Lett.* **2012**, *101*, 1016. [CrossRef]

56. Meng, P.; Deng, S.; Lu, X.; Du, Z.; Wang, B.; Huang, J.; Wang, Y.; Gang, Y.; Xing, B. Role of air bubbles overlooked in the adsorption of perfluorooctanesulfonate on hydrophobic carbonaceous adsorbents. *Environ. Sci. Technol.* **2014**, *48*, 13785–13792. [CrossRef]

57. Meng, P.; Deng, S.; Wang, B.; Huang, J.; Wang, Y.; Yu, G. Superhigh adsorption of perfluorooctane sulfonate on aminated polyacrylonitrile fibers with the assistance of air bubbles. *Chem. Eng. J.* **2017**, *315*, 108–114. [CrossRef]

58. Gungoren, C.; Ozdemir, O.; Wang, X.; Ozkan, S.G.; Miller, J.D. Effect of ultrasound on bubble-particle interaction in quartz-amine flotation system. *Ultrason. Sonochem.* **2019**, *52*, 446–454. [CrossRef]

59. Liu, W.; Pawlik, M.; Holuszko, M. The role of colloidal precipitates in the interfacial behavior of alkyl amines at gas-liquid and gas-liquid-solid interfaces. *Miner. Eng.* **2015**, *72*, 47–56. [CrossRef]

60. Zhou, S.; Zhou, W.; Dong, L.; Peng, Y.; Xie, G. Micellization transformations of sodium oleate induced by gas nucleation. *Langmuir* **2021**, *37*, 9701–9710. [CrossRef]

61. Yasui, K.; Tuziuti, T.; Kanematsu, W. Interaction of bulk nanobubbles (ultrafine bubbles) with a solid surface. *Langmuir* **2021**, *37*, 1674–1681. [CrossRef] [PubMed]

62. Zhou, W.; Liu, X.; Long, Y.; Xie, G.; Chen, Y. Monitoring effects of hydrodynamic cavitation pretreatment of sodium oleate on the aggregation of fine diaspore particles through small-angle laser scattering. *Ultrason. Sonochem.* **2023**, *100*, 106574. [CrossRef] [PubMed]